A *Picea crassifolia* Tree-Ring Width-Based Temperature Reconstruction for the Mt. Dongda Region, Northwest China, and Its Relationship to Large-Scale Climate Forcing

Yu Liu[1,2,3]*, Changfeng Sun[1,2], Qiang Li[2,3], Qiufang Cai[2]

1 Department of Earth and Environmental Science, School of Human Settlements and Civil Engineering, Xi'an Jiaotong University, Xi'an, 710049, China, **2** The State Key Laboratory of Loess and Quaternary Geology, Institute of Earth Environment, Chinese Academy of Sciences, Xi'an, 710061, China, **3** Joint Center for Global Change Studies (JCGCS), Beijing Normal University, Beijing, 100875, China

* liuyu@loess.llqg.ac.cn

Abstract

The historical May–October mean temperature since 1831 was reconstructed based on tree-ring width of Qinghai spruce (*Picea crassifolia* Kom.) collected on Mt. Dongda, North of the Hexi Corridor in Northwest China. The regression model explained 46.6% of the variance of the instrumentally observed temperature. The cold periods in the reconstruction were 1831–1889, 1894–1901, 1908–1934 and 1950–1952, and the warm periods were 1890–1893, 1902–1907, 1935–1949 and 1953–2011. During the instrumental period (1951–2011), an obvious warming trend appeared in the last twenty years. The reconstruction displayed similar patterns to a temperature reconstruction from the east-central Tibetan Plateau at the inter-decadal timescale, indicating that the temperature reconstruction in this study was a reliable proxy for Northwest China. It was also found that the reconstruction series had good consistency with the Northern Hemisphere temperature at a decadal timescale. Multi-taper method spectral analysis detected some low- and high-frequency cycles (2.3–2.4-year, 2.8-year, 3.4–3.6-year, 5.0-year, 9.9-year and 27.0-year). Combining these cycles, the relationship of the low-frequency change with the Pacific Decadal Oscillation (PDO), North Atlantic Oscillation (NAO) and Southern Oscillation (SO) suggested that the reconstructed temperature variations may be related to large-scale atmospheric-oceanic variations. Major volcanic eruptions were partly reflected in the reconstructed temperatures after high-pass filtering; these events promoted anomalous cooling in this region. The results of this study not only provide new information for assessing the long-term temperature changes in the Hexi Corridor of Northwest China, but also further demonstrate the effects of large-scale atmospheric-oceanic circulation on climate change in Northwest China.

Introduction

The Hexi Corridor is the most important grain production base and cash crop area in Northwest China [1]. Under the background of global warming, the temperature of the Hexi Corridor is unusually warm, resulting in deterioration of the ecological environment and transformation of the layout and structure of agricultural production [2]. The northern and southern mountains of the Hexi Corridor play an important role in the ecology and climate change of the corridor and its surrounding areas [3]. Therefore, it is obviously significant to understand the characteristics of climatic change with respect to these mountains. However, the instrumental data around the corridor feature only short time records that are insufficient for capturing the regularity and mechanisms of climate; therefore, paleoclimatic studies are critically important [4–6].

With its precise dating, high continuity, high resolution and easily obtained duplicates, the dendroclimatology approach is significant in studying paleoclimatic changes [7–11]. In recent decades, dendroclimatology has achieved important development in China [12–22]. There have been some climate reconstructions based on tree-ring indices in the Hexi Corridor and its vicinity, but these studies were mainly confined to the southern mountains, such as the Qilian Mountains, and most studies mainly focused on precipitation reconstruction [23–27]. Only one precipitation series was reconstructed using tree-ring indices in the northern mountainous region [28]. It remains unclear whether the trees in the northern mountains only reflect the precipitation signal and whether the climate change is similar to that in the southern mountains. Additionally, the question of whether the regional climate change regime around the Hexi Corridor is consistent on a long-term scale also remains unresolved. Therefore, it is essential to perform more dendroclimatological studies in the northern mountains of the Hexi Corridor. In this research, we selected Qinghai spruce (*Picea crassifolia* Kom.) from Mt. Dongda, which is located to the north of the Hexi Corridor, to build a tree-ring chronology for Mt. Dongda, to investigate the climatic response of the chronology and reconstruct the temperature since 1831, and to reveal the connections of the reconstructed temperature to large-scale climate forcing, including the Southern Oscillation (SO), North Atlantic Oscillation (NAO), Pacific Decadal Oscillation (PDO) and major volcanic eruptions.

Materials and Methods

Site description and tree-ring data

With the permission of the Nature Reserve Station of the Dongda Mountains, samples were collected from Mt. Dongda (39°03′N, 100°46′E), located to the North of the Hexi Corridor (Fig 1). In this region, the mean annual temperature is 4.9°C, and the annual precipitation varies widely at different altitudes. The annual precipitation is approximately 150–190 mm at elevations of less than 2200 m and 300–400 mm at elevations of 2400–3600 m [29]. Because Qinghai spruce is an ombrophyte, we selected sampling sites on the northern slopes at elevations between 2900 and 3200 m. The soils of the sites are mainly mountain gray cinnamon soils that have a high water content. The vegetation coverage (shrubs and trees) is greater than 0.8, and the dominant tree species is Qinghai spruce. To minimize non-climatic effects on tree growth, only healthy trees with little evidence of fire or human disturbance were selected. A total of 66 cores from 36 living trees were ultimately sampled using 5-mm increment borers. The group of samples was named DD.

Chronology development

In the laboratory, all the tree-ring cores were naturally dried, mounted, surfaced, and cross-dated following standard dendrochronological procedures [30]. The quality of cross-dating
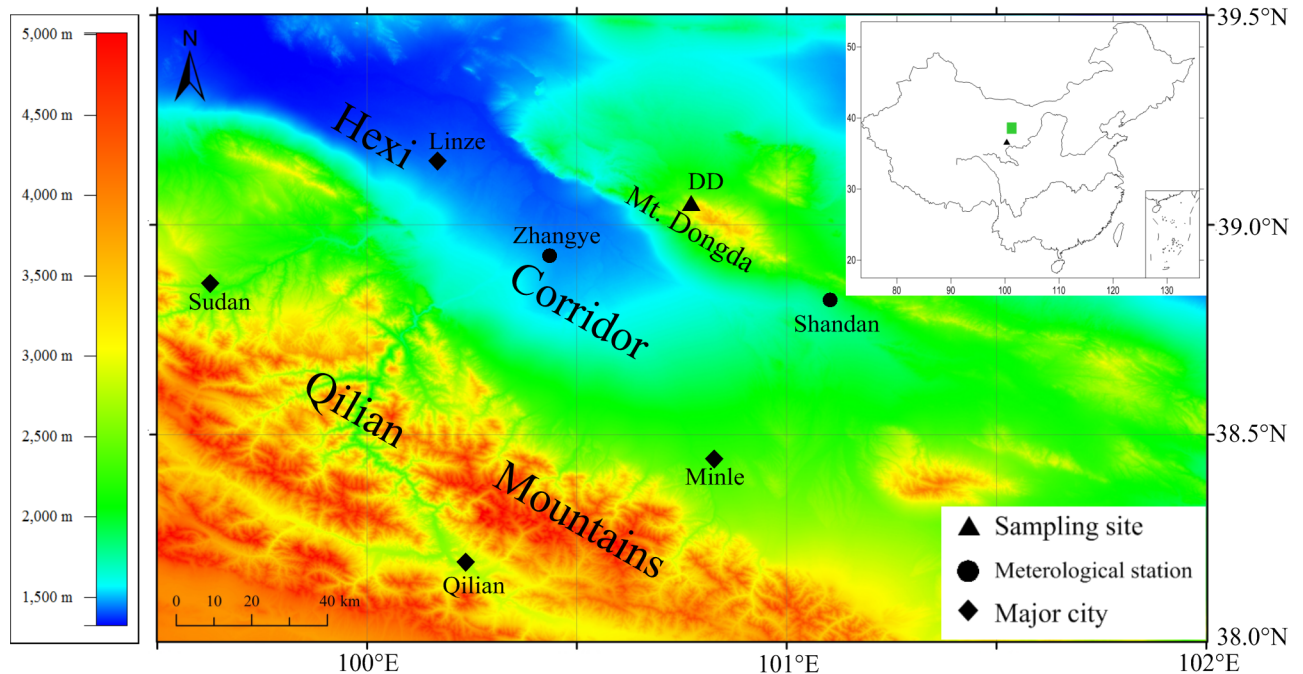
Fig 1. Location map of the tree-ring sampling sites and meteorological stations. The black triangle in the small picture in the upper right is the site used for comparison in this study.

was controlled using the COFECHA program [31] (http://www.ldeo.columbia.edu/tree-ring-laboratory/resources/software). Cores with ambiguous results and those that were too short were excluded from further analysis, and 60 cores from 35 trees were used to establish the chronology. The results from the COFECHA program showed that the mean correlation coefficient of each series with a master series was 0.66 and the mean sensitivity was 0.21.These data indicated that the ring width variation pattern of each series was relatively similar.

The CRUST program [32] (http://www.ldeo.columbia.edu/tree-ring-laboratory/resources/software) was used for detrending and developing of the tree-ring chronologies with the selection of "curve-fit detrend". Three types of chronologies could be obtained: standardized (STD), residual (RES), and autoregressive standardized (ARS). In further analysis, the STD chronology was used because it preserved both low- and high-frequency information. The expressed population signal (EPS) can be used to evaluate the reliability of the tree-ring chronology [33]. In general, the greater the sample size, the higher the EPS values. An EPS value above 0.85 is generally regarded as satisfactory [34]. In this research, an EPS value exceeding 0.85 existed after AD 1831 and corresponded to 12 trees (Fig 2).

Meteorological data

There are two meteorological stations near the sampling site: Zhangye (38°56′N, 100°26′E; elevation 1483 m; covering the period of 1951–2011) and Shandan (38°48′N, 101°05′E; elevation 1765 m; covering the period of 1953–2011). The monthly mean temperature and total precipitation of each station are shown in Fig 3. The monthly variation patterns for the two climate factors were almost synchronous between the two meteorological stations. Preliminary analyses showed that random errors and obvious uneven distributions for the climate data were not present in the meteorological records, thereby revealing that the records were reliable. Because
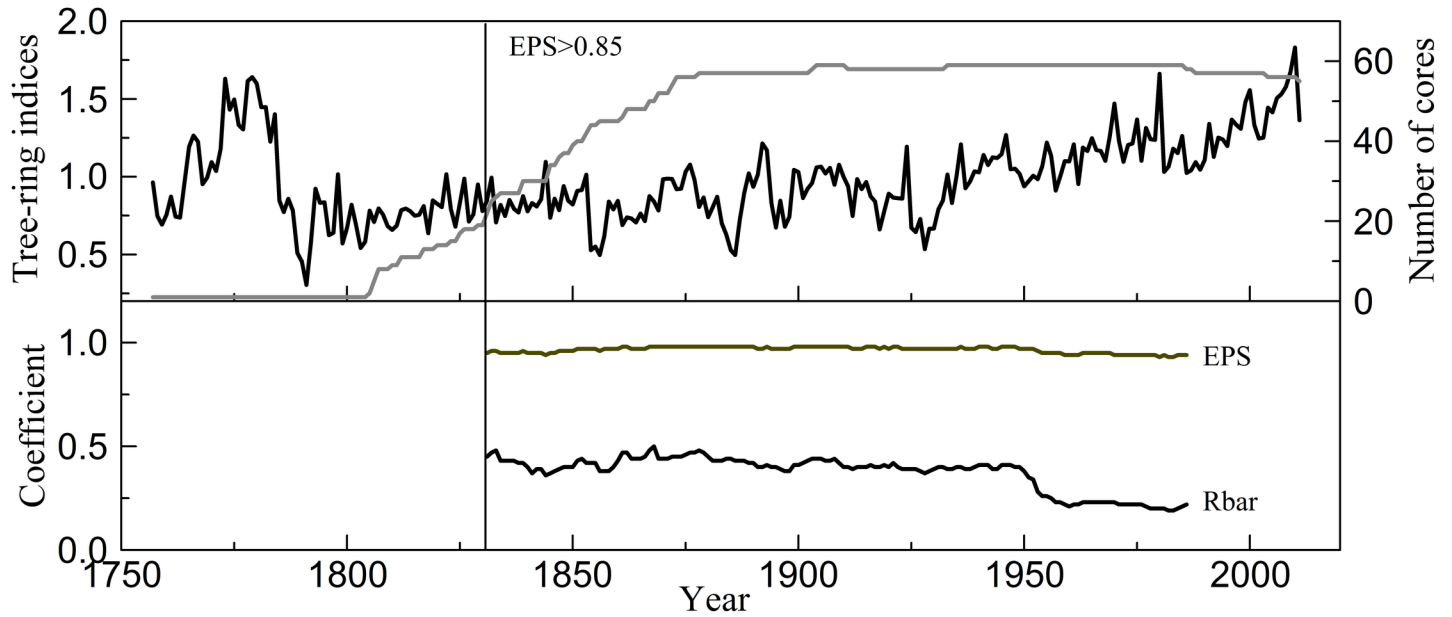
Fig 2. Tree-ring STD chronology and sample size and the running EPS and Rbar.

doi:10.1371/journal.pone.0160963.g002
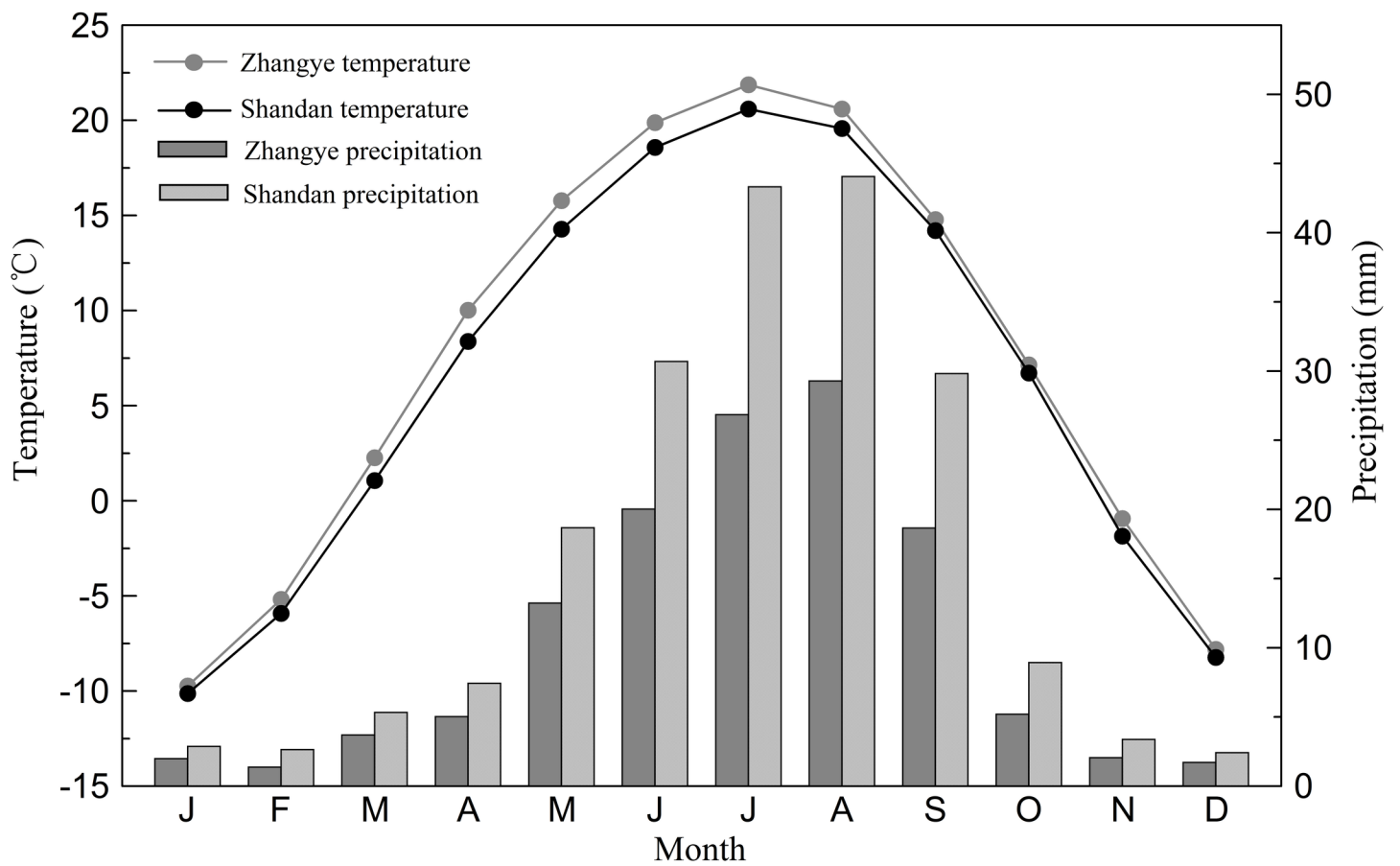
Fig 3. Monthly mean temperature and total precipitation at Zhangye (1951–2011) and Shandan (1953–2011) meteorological stations.

doi:10.1371/journal.pone.0160963.g003

the Zhangye meteorological station is closer to the sampling site and has a relatively long record period, the climatic data from this station were used for further analyses in this paper.

Statistical methods

In this paper, Pearson's correlation analyses were used to identify climate-growth relationships between the tree-ring width indices and climate data from the observation period. Then, a simple linear regression model was used for temperature reconstruction. The bootstrap and jackknife [35] statistical methods, which have been employed in dendroclimatology [36–38], were used to check the stability of the regression model. The concept behind the bootstrap resampling technique is that the available observations of a variable contain the necessary information to construct an empirical probability distribution of any statistic of interest. The bootstrap method can provide standard errors of statistical estimators even when no theory exists. The jackknife method involves calculating the correlation of the time series after progressively removing the values for one year throughout the entire time period. Multi-taper method spectral analysis [39] was conducted to identify the periodicity in the reconstructed series. Superposed epoch analysis (SEA) [40] and the Monte Carlo test [41] were used to discuss the teleconnection between our reconstructed temperature and volcanic eruptions.

Results

Tree-ring climatic response

Because the climate of the previous year may affect tree growth in the present year [42], the response analyses were assessed using the recorded climatic variables from August of the previous year to October of the present year (Fig 4). The correlation function results showed that the DD ring width had a significant correlation with precipitation in the previous and present
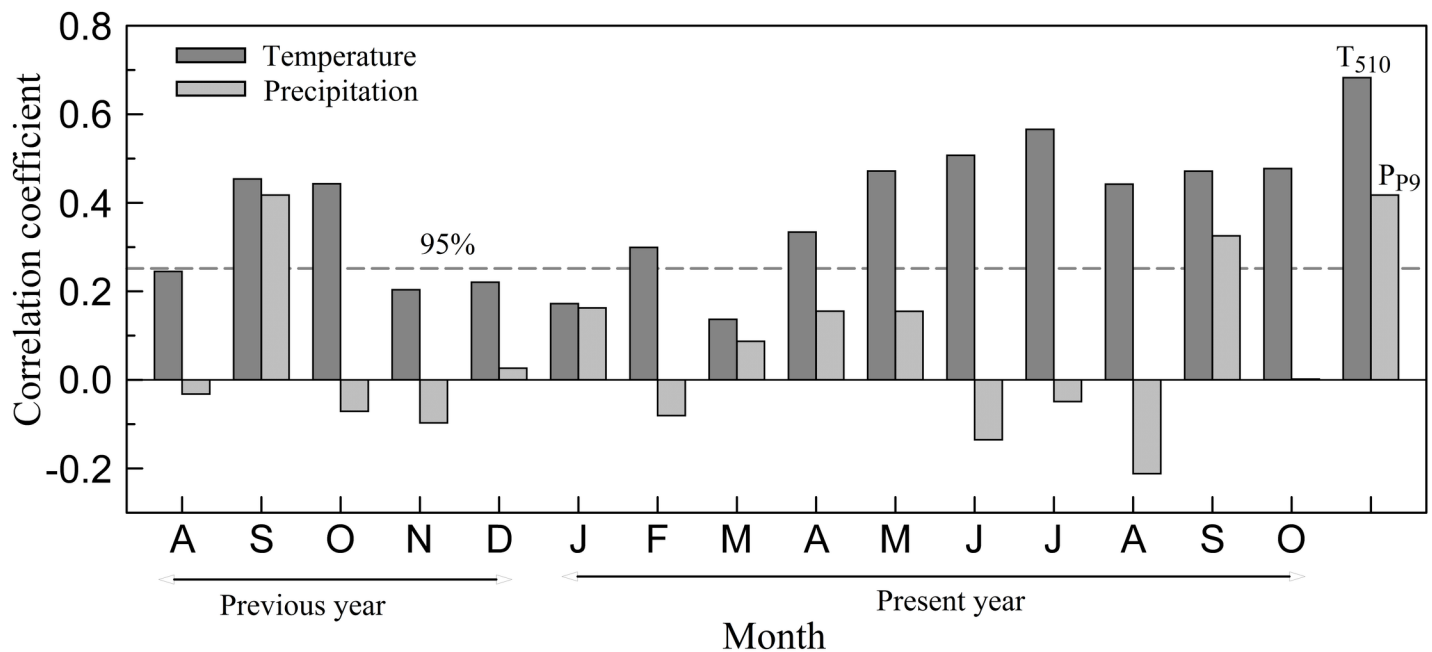
Fig 4. Correlation between tree-ring chronology and climatic records for 1951–2011. T_{510} is the mean temperature from May to October of the present year. P_{P9} is the monthly precipitation of the previous September.

doi:10.1371/journal.pone.0160963.g004

September. In contrast, the correlations between temperature and tree growth were significantly positive and exceeded the 95% significance level for most months. Generally, seasonal climate is more meaningful and stable than that of a single month. After combining the monthly data on all aspects of the climatic conditions, the months with the highest correlations for the mean temperature were those from May to October (r = 0.683) (Fig 4). The months from May to October are close to the growing season (from June to early October) of Qinghai spruce in the Mt. Dongda area [43]. During these months, higher temperatures may promote photosynthesis and generate larger rings. Based on the analyses above, it made sense that the May–October mean temperature was the limiting factor for the radial width of Qinghai spruce growing on Mt. Dongda. This result suggested that the climate signal contained in the tree-ring width from the northern mountains was different from that of the southern mountains [23–27]. This was likely because of the different climates between these mountains. Based on the same tree species and a similar sampling site, it has been previously found that precipitation was the dominant factor controlling Qinghai spruce growth on Mt. Dongda [28], which was different from our result. This was likely because RES chronology was used in that study. It is known that RES chronology conserves much higher frequency signals [34] and is usually used to reconstruct past hydroclimate changes [23, 28, 44–46].

Transfer function

Based on the above analyses, the temperature from May to October was reconstructed from the DD tree rings using the following linear regression model: $T_{510} = 2.799{*}W_t + 13.163$, (r = 0.683; $R^2 = 0.466$; $R^2_{adj} = 0.457$; F = 51.465; p<0.0001; D/W = 1.202), where T_{510} is the mean temperature from May to October (1951–2011), and W_t represents the index of the STD tree-ring width chronology.

The test results of the robustness and reliability of the relationship between the chronology and the May–October mean temperature are shown in Table 1. Both the bootstrap and jackknife methods generated similar statistical results for the calibration period, suggesting that the temperature reconstruction was stable and reliable. In addition, Fig 5A showed that the reconstruction closely tracked the observed temperature.

May–October mean temperature reconstruction

Using the above transfer function, we reconstructed the May–October mean temperature history since 1831 (Fig 5B, see data in S1 Text). During the reconstructed interval (1831–2011), the mean T_{510} was 15.64°C, and the standard deviation (σ) was 1.00°C.

Table 1. Verification results of the bootstrap and jackknife methods for May–October temperature reconstruction.

Statistical items	Calibration period (1951–2011)	Verification period (1951–2011)	
		Bootstrap (100 iterations) mean (range)	Jackknife mean (range)
r	0.683	0.67 (0.47–0.84)	0.68 (0.63–0.73)
R^2	0.466	0.46 (0.22–0.71)	0.47 (0.40–0.53)
R^2_{adj}	0.457	0.45 (0.21–0.70)	0.46 (0.39–0.52)
SE	0.581	0.57 (0.40–0.72)	0.58 (0.55–0.58)
F	51.465	54.46 (17.04–142.38)	50.69 (38.66–64.23)
P	<0.0001	<0.0001	<0.0001
D/W	1.202	2.01 (1.18–2.60)	1.21 (1.11–1.38)

doi:10.1371/journal.pone.0160963.t001
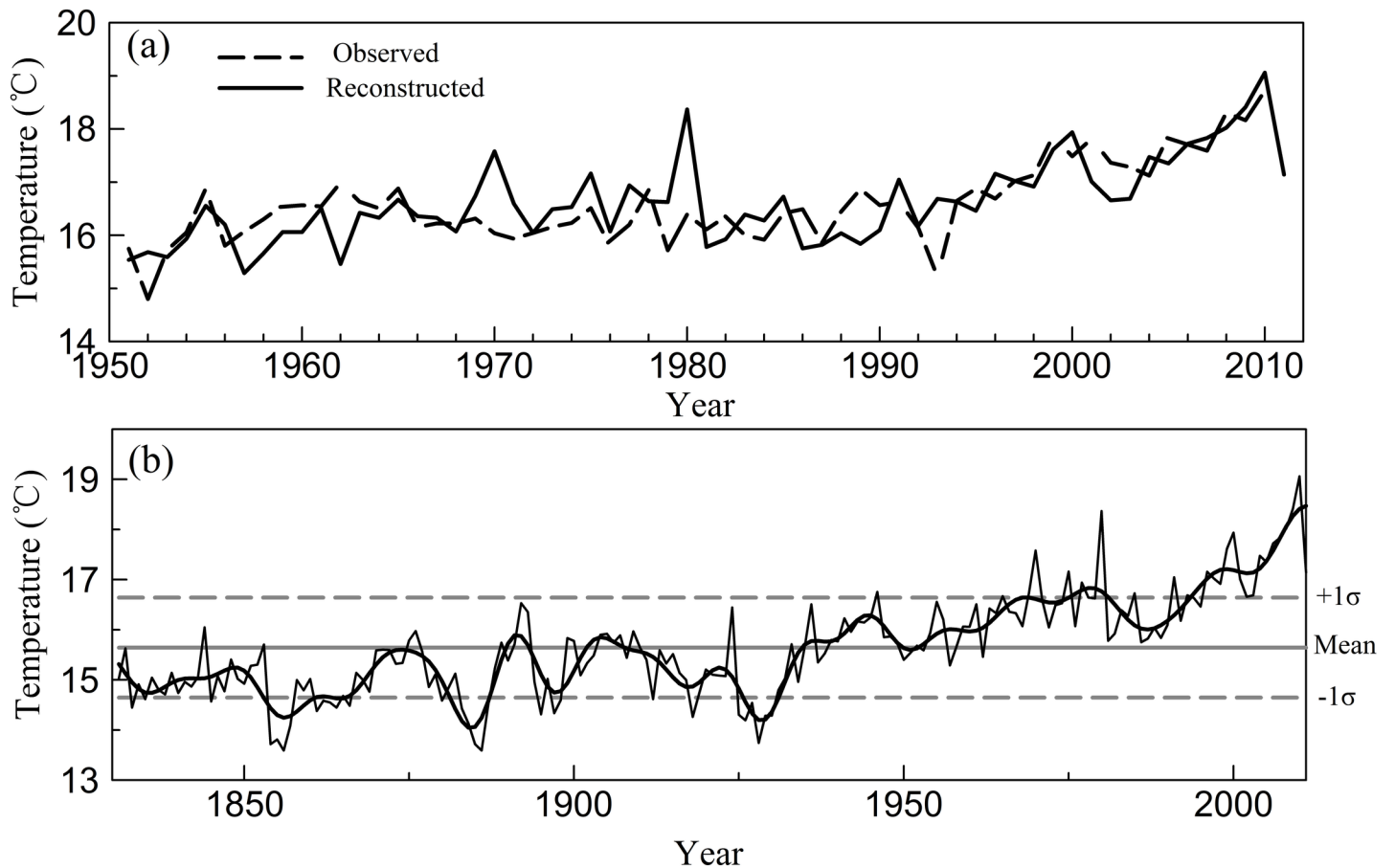
Fig 5. The observed and reconstructed May–October mean temperature (T$_{510}$). (a) Comparison between observed and reconstructed T$_{510}$ for their common period of 1951–2011 and (b) T$_{510}$ reconstruction for Mt. Dongda since 1831. The thick line in (b) shows the smoothed data with a 10-year low-pass filter. The solid horizontal line represents the long-term mean for the period of 1831–2011; the dashed horizontal lines represent the mean value ± 1σ.

Periodicity analysis for the reconstructed temperature

Multi-taper method spectral analysis [39] was conducted to identify the periodicities in the reconstructed series. The results showed that the reconstructed temperature for Mt. Dongda contained significant periodicities at 2.3–2.4-year, 2.8-year, 3.4–3.6-year, 5.0-year, 9.9-year and 27.0-year (Fig 6).

Discussion

May–October mean temperature variations

To investigate historical temperature changes, we defined a warm year as >mean+1σ (16.64°C) and a cold year as <mean−1σ (14.64°C). The full reconstruction of the mean temperature displayed strong interannual variability from 1831 to 2011. During the last 181 years, 27 warm years and 29 cold years occurred in the reconstruction series. These warm and cold years accounted for 14.92% and 16.02% of the total, respectively. The twenty warmest/coldest years, with their T$_{510}$ values, are shown in Table 2.

To analyze the low-frequency variation of the reconstruction, a 10-year low-pass filter was applied (Fig 5B). After smoothing, the entire reconstructed temperature curve presented four warm periods (1890–1893, 1902–1907, 1935–1949 and 1953–2011) with temperatures higher
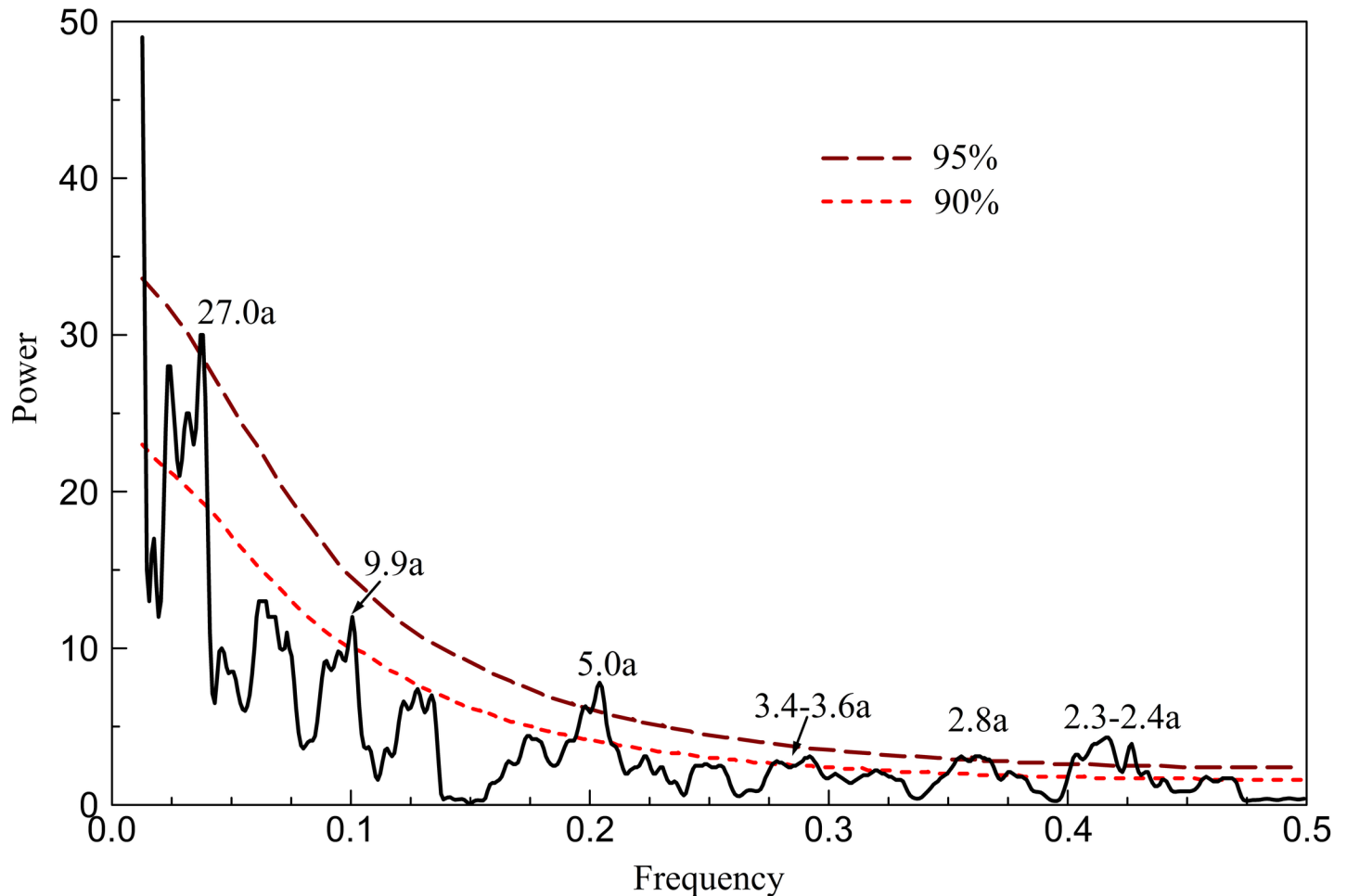
Fig 6. Spectrum analysis result of the reconstructed mean temperature. The dashed line indicates the 95% and 90% confidence levels.

than the mean, and four cold periods (1831–1889, 1894–1901, 1908–1934 and 1950–1952) with temperatures lower than the mean. Among them, the interval 1953–2011 was the longest warm period, and 1831–1889 was the longest cold period in the reconstructed period. There was an obvious warming trend in the last twenty years. In addition, this warming trend has also been observed widely in other dendroclimatological studies in China [47–50]. The 10-year low-pass filtering series also showed that there were three colder periods (1853–1860, 1882–1887, 1926–1931) with temperatures lower than the mean−1σ and two warmer periods (1975–1981, 1994–2011) with temperatures higher than the mean+1σ.

Comparison with other tree-ring-based temperature reconstructions

The reconstructed temperature series in this study provides useful information for analyzing climate change in the Hexi Corridor. Due to the lack of temperature reconstructions from areas around the research region, we compared our reconstruction with a tree-ring-based temperature reconstruction from Wulan-Dulan, in the east-central Tibetan Plateau [16, 51], to evaluate the reliability of the reconstruction. Both series were smoothed using a 10-year low-pass filter (Fig 7A and 7B). The reconstructed temperature series for Mt. Dongda correlates well with the temperature series of Wulan-Dulan with r = 0.55 (p<0.001, n = 170) on an

Table 2. The twenty warmest/coldest years in the reconstructed May–October mean temperature series (T_{510}).

Rank	Warmer year	T_{510} (°C)	Colder year	T_{510} (°C)
1	2010	19.06	1856	13.59
2	2009	18.41	1886	13.59
3	1980	18.37	1854	13.72
4	2008	18.02	1885	13.72
5	2000	17.94	1928	13.74
6	2007	17.83	1855	13.81
7	2006	17.72	1857	14.09
8	1999	17.61	1884	14.13
9	1970	17.58	1926	14.19
10	2004	17.47	1918	14.26
11	2005	17.35	1929	14.28
12	1975	17.16	1930	14.29
13	1996	17.16	1925	14.30
14	2011	17.14	1895	14.31
15	1991	17.05	1897	14.34
16	1997	17.02	1861	14.38
17	2001	17.01	1883	14.43
18	1977	16.94	1833	14.45
19	1998	16.92	1864	14.45
20	1946	16.76	1866	14.48

doi:10.1371/journal.pone.0160963.t002

annual scale and r = 0.67 (p<0.01, n = 17) on a decadal scale. Comparisons between these series revealed that the warm/cold variations were coherent with the low-frequency data at the large scale. These two series contained the same cooling/warming periods. Starting in the 1930s, both series exhibited a significant warming trend. Of course, there were nonconformities in these series during some periods, which may have been caused by possible differences in microhabitats at the sampling site and/or the reconstruction of different seasonal periods. On the whole, the results indicated that the Mt. Dongda tree-ring index reflected the temperature history not only of the study area, but also of the larger region of Northwest China.

Further analysis indicated that our reconstructed temperature exhibited changes on the long-term scale that are similar to those of the Northern Hemisphere (NH) temperature. The reconstructed temperature was significantly correlated with the NH temperature reconstruction [10, 52–56]. The correlation coefficients ranged from 0.44 to 0.59 (p<0.001, n>150). In addition, there was also a remarkable relationship between our temperature and the NH mean May–October temperature observations (r = 0.60, 1880–2011, p<0.0001). After application of a 10-year low-pass filter, the low-frequency changes appeared to be coherent among these temperature series (Fig 7C). These findings indicated that there was good consistency between the temperature of Mt. Dongda and the NH temperature at a low-frequency change and also suggested that our reconstructed series could be used as a proxy for other researchers to reconstruct large-scale regional temperature, such as the NH temperature.

Teleconnections with SO, PDO and NAO

It was reported that the SO had effects on the temperature variations in China [57]. By comparing the temperature history with August–September observations of the Southern Oscillation Index (SOI) series, we found that the two series had a significant relationship following the
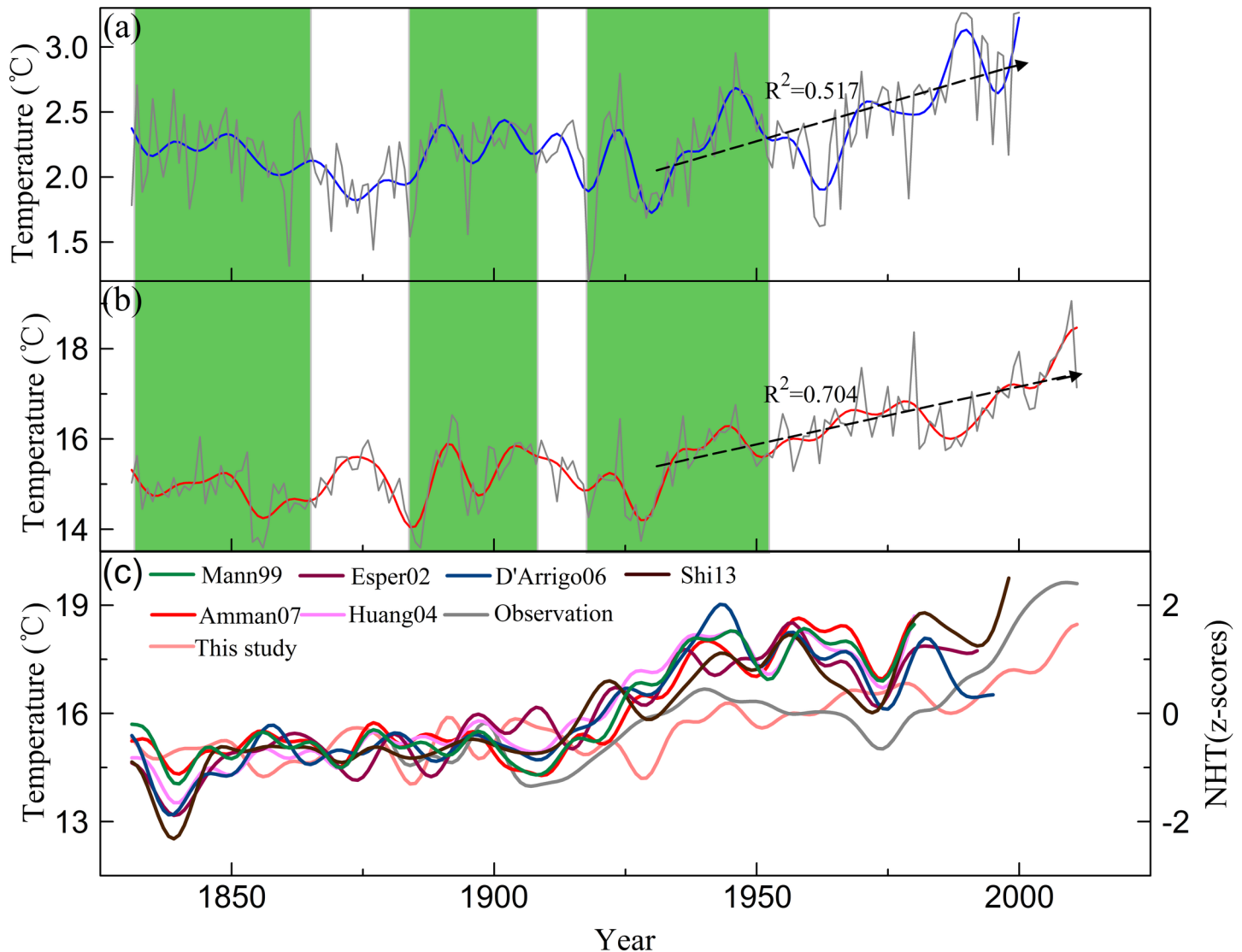
Fig 7. Comparison between the mid-eastern Tibetan Plateau temperature (a), the reconstructed temperature (b), and the NH temperature (c). All time series were smoothed using a 10-year low-pass filter. Vertical bars in (a) and (b) indicate when the two temperature series are in-phase, and the dashed line with an arrow indicates the linear fitting values during the period 1931–2011.

doi:10.1371/journal.pone.0160963.g007

application of a 20-year low-pass filter (Fig 8). In addition to this, the 2.3–2.4-year, 2.8-year, 3.4–3.6-year and 5.0-year cycles of our temperature reconstruction also existed in the SOI [58]. These results might imply possible impacts of the SO on temperature in our study region, and the ring width of Qinghai spruce on Mt. Dongda may contain an SO signal. During a strong negative-phase of SO with El Niño developing, an anomalous descending motion appeared in the western Pacific [59], which could cause a large variability in the East Asian Summer Monsoon (EASM). The anomalous cyclonic circulation (with strong anomalous westerly winds) over the western Pacific reflected a weak western Pacific sub-tropical high in the El Niño developing summer. This resulted in the weakened EASM, which does not benefit the temperature in Northwest China [60].

The cycles at 9.9-year and 27.0-year may correspond to the PDO and NAO [61, 62], because there were also significant correlations between the temperature and the PDO and NAO. The
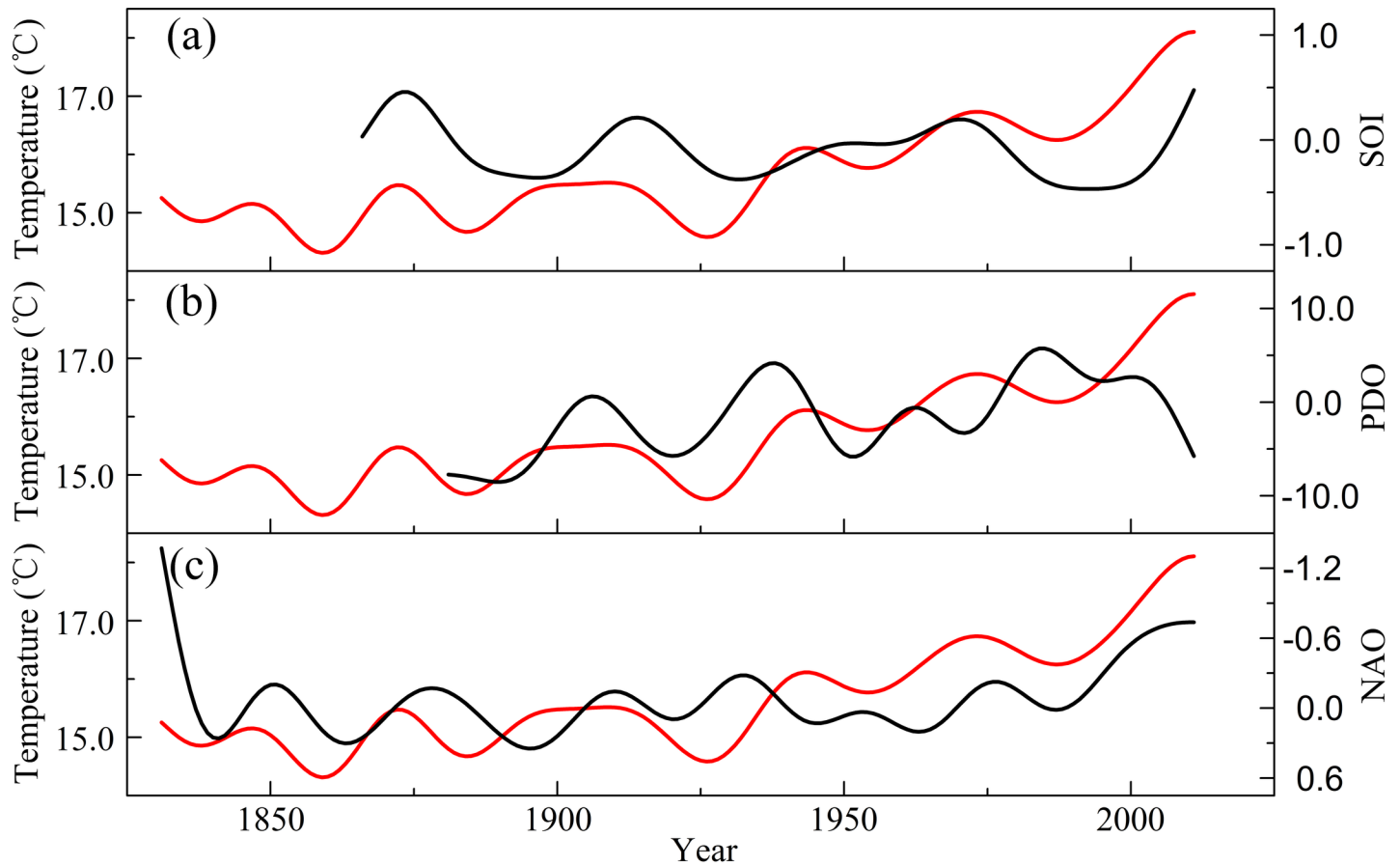
Fig 8. Comparison between our reconstructed temperature and the large-scale atmospheric-oceanic circulations (SO, PDO and NAO). These were smoothed using a 20-year low-pass filter.

doi:10.1371/journal.pone.0160963.g008

correlation coefficient between the reconstructed temperature and the observed PDO index from the previous October to the present March at an interannual scale is 0.27 ($p<0.005$, 1881–2011). The correlation coefficient between the reconstructed temperature and the April–September NAO index is -0.20 ($p<0.01$, 1831–2011). In addition, after application of a 20-year low-pass filter, our temperature fluctuates synchronously with PDO and inversely with NAO at most time intervals. Moreover, these cycles appear widely in the tree-ring record of Northwest China [63, 64]. This may suggest that the temperature variability in Northwest China is partly influenced by large-scale circulation features, such as the NAO and PDO. The above analysis indicates that the effect of SO and NAO on the temperature of Northwest China is seasonally similar and the influence of PDO is seven months ahead. Previous work [59] showed that during a warm PDO phase in the winter, the Mongolian High strengthened and the Siberian High was weakened, which indicated an interdecadal seesaw-like oscillation between the two pressure systems. This pattern implied that the cold wind from Siberia tended to be weaker, and the air temperature was higher in Northwest China [65, 66]. A positive (negative) summer (July–September) NAO (SNAO) leads to a strong lower-level divergence (convergence) over the Asian jet entrance region, which in turn excites a strong upper-level convergence (divergence) driven by Ekman pumping [67, 68]. Such a convergence (divergence) then stimulates a zonally oriented quasi-stationary barotropic Rossby wave train along the Asian

upper-level jet. Therefore, the SNAO signal is transported eastward to East Asia, resulting in an anomalous summer air temperature over Northwest China [69].

Linkages with volcanic eruptions

Large volcanic eruptions inject sulfur gases into the stratosphere, which are converted to sulfate aerosols with an e-folding residence timescale of approximately one year. The climate response to large eruptions lasts for several years [70]. These phenomena can be recorded by reconstructed temperature series based on tree rings [71, 72]. We employed a historical/geological record based on the volcanic explosivity index (VEI) [73] that accurately records volcanic eruptions. The VEI value for each volcanic event was obtained from http://www.volcano.si.edu/search_eruption_results.cfm.

Before assessing the possible relationship, the reconstructed temperature was processed using a 10-year high-pass filter to highlight the interannual variability. The comparison of our reconstruction with large eruptions (VEI $\geq$4) revealed that the Mt. Dongda temperature decreased in association with volcanic eruptions. The 26 cold years, which were defined as temperature <mean−1σ, almost all occurred after volcanic eruptions (Fig 9A). To clarify this point further, we used the SEA method [40] to assess the relationship between the volcanic eruptions (VEI >4) and the reconstructed temperature for the past 181 years. Through simple compositing, the SEA method involves sorting data into categories dependent on a 'key-date' for synchronization and then comparing the means of those categories. Given sufficient data, a common underlying (causal) response to a forcing event should theoretically emerge in the average (composite) while other noise in the data should be cancelled [40]. The annual composites of the SEA results in the year +1 passed the 90% significant level test based on the Monte Carlo test [41]. The results indicated that anomalous cooling on Mt. Dongda occurred in one year after eruption (Fig 9B). The radiative effects of this aerosol cloud resulting from major eruptions can induce substantial global cooling, which may influence regional temperature change by atmospheric circulation [70]. Using observed data, it was previously found that large explosive volcanic eruptions could result in a decrease in surface temperature over almost all parts of China [74], which had a time lag of approximately one year. In general, major volcanic eruptions play an important role in high-frequency temperature change in Northwest China.

The effects of volcanic eruptions on climate change were possibly via large-scale atmospheric-oceanic variations [59]. It has been previously found that volcanic eruptions had directly impact on the El Niño/Southern Oscillation (ENSO) variation [75]. In order to clearly explain the relationships among volcanic eruptions, ENSO and temperature change in Northwest China, the SEA method was also used to analyze the relationships between temperature variation and the most negative ENSO years since 1831 [75], where the most negative ENSO years were those with values lower than the mean−1σ of the whole ENSO series. The results showed that anomalous cooling occurred in the year with more negative ENSO (Fig 9C). The reconstructed ENSO was the previous November–January Niño3.4 index and immediate cooling tended to occur in the Niño3.4 Pacific region in the year of eruption [75]. Combined with the SEA results (Fig 9B and 9C), we inferred that volcanic eruption influenced the Niño3.4 index from the November of the eruption year to the next January which affected the following May–October temperature of Northwest China; therefore, anomalous cooling occurred in one year after eruption.

Conclusions

The May–October mean temperature history since 1831 was reconstructed based on tree-ring width chronology of Qinghai spruce from Mt. Dongda, which is located to the North of the
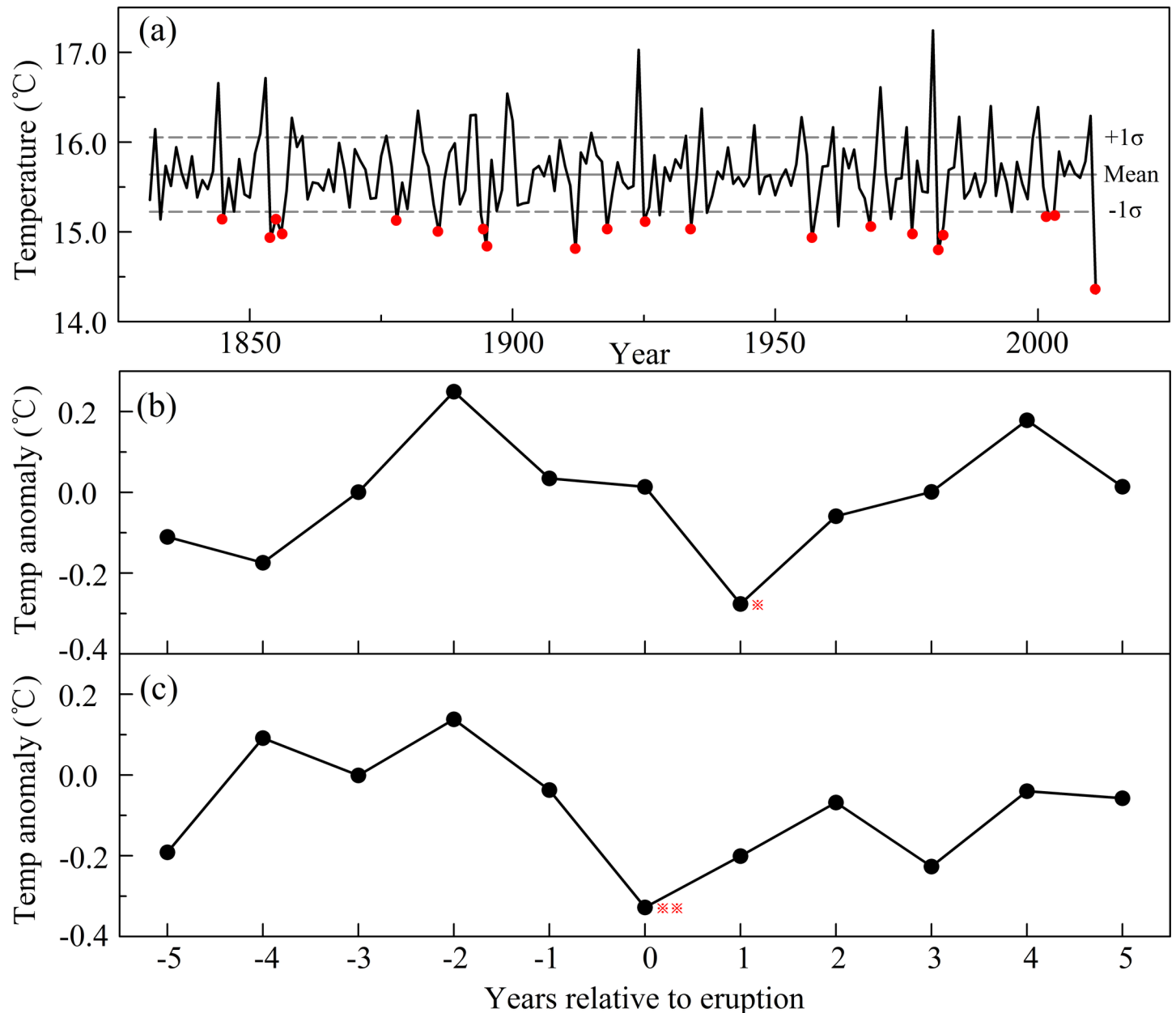
Fig 9. The connection between reconstructed temperature, major volcanic eruptions and the most negative ENSO years. (a) The corresponding relationship between the reconstructed temperature filtered using a 10-year high-pass filter and volcanic eruptions. The solid horizontal line represents the long-term mean of the filtered temperature for the period of 1831–2011; the dashed horizontal lines represent the mean value ± 1σ. The solid cycles indicate a cold year following a volcanic eruption event. (b) The filtered temperature superposed epoch analysis (SEA) [40] results for (b) the major volcanic eruptions (VEI >4) and (c) the most negative ENSO years [75] since 1831. One and two asterisks denoted anomalies significant at the 0.1 and 0.05 levels, respectively, based on the Monte Carlo test [41].

doi:10.1371/journal.pone.0160963.g009

Hexi Corridor in Northwest China. This reconstruction accounted for 46.6% of the variance of the observed temperature over the period of 1951–2011, and the transform function was verified as stable and reliable. During the reconstruction history from 1831 to 2011, there were 27 warm and 29 cold years. The entire reconstructed temperature series presented four warm periods (1890–1893, 1902–1907, 1935–1949 and 1953–2011) and four cold periods (1831–1889, 1894–1901, 1908–1934 and 1950–1952) at a low-frequency change. The longest warm and cold

periods occurred during 1953–2011 and 1831–1889, respectively. Through comparison with the east-central Tibetan Plateau temperature series reconstructed using Wulan-Dulan tree rings, we found the two series presented similar warm/cold variations in some periods, indicating that the temperature variation in this study is a reliable proxy for Northwest China. Furthermore, our reconstruction also has good consistency with the NH temperature at a low-frequency change. Spectral analysis showed that the temperature variation in this region had significant periodicities at 2.3–2.4-year, 2.8-year, 3.4–3.6-year, 5.0-year, 9.9-year and 27.0-year, which are related to the SO, PDO or NAO. Combining the correlation and comparison analysis, it is suggested that the SO, PDO and NAO might partly influence the temperature variation in the Hexi Corridor of Northwest China, especially the low-frequency change. Almost all cold years in the high-pass-filtered temperature reconstruction coincided with major volcanic eruptions. These eruptions promoted anomalous cooling in the study region. The preliminary results presented in this paper provide new information on the long-term temperature changes in the Hexi Corridor of Northwest China and demonstrate the effects of large-scale atmospheric-oceanic circulation on climate change in Northwest China.

Supporting Information

S1 Text. Temperature reconstruction for the Mt. Dongda region, Northwest China. The data includes the reconstructed May–October mean temperature series.
(TXT)

Acknowledgments

Author Contributions

Conceptualization: YL.

Data curation: YL CFS QFC.

Funding acquisition: YL CFS.

Investigation: YL CFS QL.

Methodology: YL CFS.

Project administration: YL CFS.

Resources: CFS QL QFC.

Software: CFS.

Supervision: YL.

Visualization: YL CFS.

Writing - original draft: CFS.

Writing - review & editing: YL CFS QL QFC.

References

1. Guo XQ, Liu MC (2011) Spatiotemporal characteristics of climate productivity potential during last 40 years in the Hexi Corridor. Journal of Desert Reseach 31: 1323–1329. [in Chinese, with English abstract]

2. Yin XL, Hao ZY, Wei F, Dai DB (2008) Influence of climate warming on agriculture in the middle of Hexi Corridor. Arid Meteorology 26: 90–94. [in Chinese, with English abstract]

3. Jia WX, He YQ, Li ZS, Pang HX (2008) Spatio-temporal Distribution Characteristics of Climate Change in Qilian Mountains and Hexi Corridor. Journal of Desert Reseach 28: 1151–1155. [in Chinese, with English abstract]

4. Cook ER, Esper J, D'Arrigo RD (2004) Extra-tropical Northern Hemisphere land temperature variability over the past 1000 years. Quaternary Science Reviews 23: 2063–2074.

5. D'Arrigo R, Mashig E, Frank D, Wilson R, Jacoby G (2005) Temperature variability over the past millennium inferred from Northwestern Alaska tree rings. Climate Dynamics 24: 227–236.

6. Mann ME, Zhang ZH, Hughes MK, Bradley RS, Miller SK, Rutherford S, et al. (2008) Proxy-based reconstructions of hemispheric and global surface temperature variations over the past two millennia. Proceedings of the National Academy of Sciences of the United States of America 105: 13252–13257. doi: 10.1073/pnas.0805721105 PMID: 18765811

7. Briffa KR, Osborn TJ, Schweingruber FH, Jones PD, Shiyatov SG, Vaganov EA (2002) Tree-ring width and density data around the Northern Hemisphere: Part 2, spatio-temporal variability and associated climate patterns. Holocene 12: 759–789.

8. Buntgen U, Tegel W, Nicolussi K, McCormick M, Frank D, Trouet V, et al. (2011) 2500 Years of European Climate Variability and Human Susceptibility. Science 331: 578–582. doi: 10.1126/science.1197175 PMID: 21233349

9. Cook ER, Anchukaitis KJ, Buckley BM, D'Arrigo RD, Jacoby GC, Wright WE (2010) Asian Monsoon Failure and Megadrought During the Last Millennium. Science 328: 486–489. doi: 10.1126/science.1185188 PMID: 20413498

10. Esper J, Cook ER, Schweingruber FH (2002) Low-frequency signals in long tree-ring chronologies for reconstructing past temperature variability. Science 295: 2250–2253. PMID: 11910106

11. Liu Y, Wang YC, Li Q, Sun JY, Song HM, Cai QF, et al. (2013) Reconstructed May-July mean maximum temperature since 1745 AD based on tree-ring width of Pinus tabulaeformis in Qianshan Mountain, China. Palaeogeography Palaeoclimatology Palaeoecology 388: 145–152.

12. Duan JP, Zhang QB, Lv LX, Zhang C (2012) Regional-scale winter-spring temperature variability and chilling damage dynamics over the past two centuries in southeastern China. Climate Dynamics 39: 919–928.

13. Gou XH, Deng Y, Chen FH, Yang MX, Gao LL, Nesje A, et al. (2014) Precipitation variations and possible forcing factors on the Northeastern Tibetan Plateau during the last millennium. Quaternary Research 81: 508–512.

14. Li JB, Gou XH, Cook ER, Chen FH (2006) Tree-ring based drought reconstruction for the central Tien Shan area in northwest China. Geophysical Research Letters 33: L07715. doi: 10.1029/2006gl025803

15. Liang EY, Shao XM, Liu HY, Dieter E (2007) Tree-ring based PDSI reconstruction since AD 1842 in the ortindag sand land, east inner mongolia. Chinese Science Bulletin 52: 2715–2721.

16. Liu Y, An ZS, Linderholm HW, Chen DL, Song HM, Cai QF, et al. (2009) Annual temperatures during the last 2485 years in the mid-eastern Tibetan Plateau inferred from tree rings. Science in China Series D-Earth Sciences 52: 348–359.

17. Liu Y, An ZS, Ma HZ, Cai QF, Liu ZY, Kutzbach JK, et al. (2006) Precipitation variation in the northeastern Tibetan Plateau recorded by the tree rings since 850 AD and its relevance to the Northern Hemisphere temperature. Science in China Series D-Earth Sciences 49: 408–420.

18. Shao X, Xu Y, Yin ZY, Liang E, Zhu H, Wang S (2010) Climatic implications of a 3585-year tree-ring width chronology from the northeastern Qinghai-Tibetan Plateau. Quaternary Science Reviews 29: 2111–2122.

19. Yang B, Qin C, Wang JL, He MH, Melvin TM, Osborn TJ, et al. (2014) A 3,500-year tree-ring record of annual precipitation on the northeastern Tibetan Plateau. Proceedings of the National Academy of Sciences of the United States of America 111: 2903–2908. doi: 10.1073/pnas.1319238111 PMID: 24516152

20. Yang FM, Wang N, Shi F, Ljungqvist FC, Wang SG, Fan ZX, et al. (2013) Multi-Proxy Temperature Reconstruction from the West Qinling Mountains, China, for the Past 500 Years. Plos One 8(2): e57638. doi: 10.1371/journal.pone.0057638 PMID: 23451254

21. Zhang QB, Cheng GD, Yao TD, Kang XC, Huang JG (2003) A 2,326-year tree-ring record of climate variability on the northeastern Qinghai-Tibetan Plateau. Geophysical Research Letters 30: 1739. doi: 10.1029/2003gl017425

22. Zhu HF, Xu P, Shao XM, Luo HJ (2013) Little Ice Age glacier fluctuations reconstructed for the southeastern Tibetan Plateau using tree rings. Quaternary International 283: 134–138.

23. Chen F, Yuan Y, Wei W (2011) Climatic response of Picea crassifolia tree-ring parameters and precipitation reconstruction in the western Qilian Mountains, China. Journal of Arid Environments 75: 1121–1128.

24. Liu Y, Sun JY, Song HM, Cai QF, Bao G, Li XX (2010) Tree-ring hydrologic reconstructions for the Heihe River watershed, western China since AD 1430. Water Research 44: 2781–2792. doi: 10.1016/j.watres.2010.02.013 PMID: 20206961

25. Sun JY, Liu Y (2012) Tree ring based precipitation reconstruction in the south slope of the middle Qilian Mountains, northeastern Tibetan Plateau, over the last millennium. Journal of Geophysical Research-Atmospheres 117: D08108. doi: 10.1029/2011jd017290

26. Tian QH, Zhou XJ, Gou XH, Zhao P, Fan ZX, Helama S (2012) Analysis of reconstructed annual precipitation from tree-rings for the past 500 years in the middle Qilian Mountain. Science China-Earth Sciences 55: 770–778.

27. Zhang Y, Tian QH, Gou XH, Chen FH, Leavitt SW, Wang YS (2011) Annual precipitation reconstruction since AD 775 based on tree rings from the Qilian Mountains, northwestern China. International Journal of Climatology 31: 371–381.

28. Chen F, Yuan YJ, Wei WS, Zhang RB, Yu SL, Shang HM, et al. (2013) Tree-ring-based annual precipitation reconstruction for the Hexi Corridor, NW China: consequences for climate history on and beyond the mid-latitude Asian continent. Boreas 42: 1008–1021.

29. Qiu MX, Chen BS (1984) The vegetation of the Dongdashan mountain area in Zhangye region. Acta Phytoecologica & Geobotanica Sinaca 8: 235–239. [in Chinese]

30. Stokes MA, Smiley TL (1996) An introduction to tree-ring dating. Tucson: The University of Arizona Press.

31. Holmes RL (1983) Computer-assisted quality control in tree-ring dating and measurement. Tree-Ring Bulletin 43: 69–78.

32. Melvin TM, Briffa KR (2014) CRUST: Software for the implementation of Regional Chronology Standardisation: Part 1. Signal-Free RCS. Dendrochronologia 32: 7–20.

33. Wigley TML, Briffa KR, Jones PD (1984) On the average value of correlated time series, with application in dendroclimatology and hydrometeorology. Journal of Climate and Applied Meteorology 23: 201–213.

34. Cook ER, Kairiukstis LA (1990) Methods of Dendrochronology. Dordrecht: Kluwer Academic Publishers.

35. Tibshirani R (1986) Jackknife, Bootstrap and Other Resampling Methods in Regression-Analysis—Discussion. Annals of Statistics 14: 1335–1339.

36. Bao G, Liu Y, Liu N (2012) A tree-ring-based reconstruction of the Yimin River annual runoff in the Hulun Buir region, Inner Mongolia, for the past 135 years. Chinese Science Bulletin 57: 4765–4775.

37. Cai Q, Liu Y, Lei Y, Bao G, Sun B (2014) Reconstruction of the March-August PDSI since 1703 AD based on tree rings of Chinese pine (Pinus tabulaeformis Carr.) in the Lingkong Mountain, southeast Chinese loess Plateau. Climate of the Past 10: 509–521.

38. Liu N, Liu Y, Bao G, Bao M, Wang YC, Ge YX, et al. (2015) A tree-ring based reconstruction of summer relative humidity variability in eastern Mongolian Plateau and its associations with the Pacific and Indian Oceans. Palaeogeography Palaeoclimatology Palaeoecology 438: 113–123.

39. Thomson DJ (1982) Spectrum Estimation and Harmonic-Analysis. Proceedings of the Ieee 70: 1055–1096.

40. Adams JB, Mann ME, Ammann CM (2003) Proxy evidence for an El Nino-like response to volcanic forcing. Nature 426: 274–278. PMID: 14628048

41. Efron B, Tibshirani R (1986) Bootstrap methods for standard errors, confidence intervals, and other measures of statistical accuracy. Statistical Science 1: 54–75.

42. Fritts HC (1976) Tree Rings and Climate. New York: Academic Press. 567 p.

43. Bai DZ (2012) The impact factors of growth and regeneration of Picea crassifolia growing at timberline in the Qilian Mountains [Ecology]. Beijing: Chinese Academy of Forestry. [in Chinese with English abstract]

44. Fan ZX, Brauning A, Cao KF (2008) Tree-ring based drought reconstruction in the central Hengduan Mountains region (China) since AD 1655. International Journal of Climatology 28: 1879–1887.

45. Lei Y, Liu Y, Song HM, Sun B (2014) A wetness index derived from tree-rings in the Mt. Yishan area of China since 1755 AD and its agricultural implications. Chinese Science Bulletin 59: 3449–3456.

46. Peng JJ, Sun Y, Chen M, He XY, Davi NK, Zhang XL, et al. (2013) Tree-ring based precipitation variability since AD 1828 in northwestern Liaoning, China. Quaternary International 283: 63–71.

47. Bao G, Liu Y, Linderholm HW (2012) April-September mean maximum temperature inferred from Hailar pine (Pinus sylvestris var. mongolica) tree rings in the Hulunbuir region, Inner Mongolia, back to 1868 AD. Palaeogeography Palaeoclimatology Palaeoecology 313: 162–172.

48. Cai QF, Liu Y, Tian H (2013) A dendroclimatic reconstruction of May-June mean temperature variation in the Heng Mounatins, north China, since 1767 AD. Quaternary International 283: 3–10.

49. Chen ZJ, Zhang XL, He XY, Davi NK, Cui MX, Peng JJ (2013) Extension of summer (June-August) temperature records for northern Inner Mongolia (1715–2008), China using tree rings. Quaternary International 283: 21–29.

50. Liu Y, Wang YC, Li Q, Song HM, Linderhlom HW, Leavitt SW, et al. (2014) Tree-ring stable carbon isotope-based May-July temperature reconstruction over Nanwutai, China, for the past century and its record of 20th century warming. Quaternary Science Reviews 93: 67–76.

51. Liu Y, Cai QF, Song HM, An ZS, Linderholm HW (2011) Amplitudes, rates, periodicities and causes of temperature variations in the past 2485 years and future trends over the central-eastern Tibetan Plateau. Chinese Science Bulletin 56: 2986–2994.

52. Ammann CM, Wahl ER (2007) The importance of the geophysical context in statistical evaluations of climate reconstruction procedures. Climatic Change 85: 71–88.

53. D'Arrigo R, Wilson R, Jacoby G (2006) On the long-term context for late twentieth century warming. Journal of Geophysical Research-Atmospheres 111: D03103. doi: 10.1029/2005jd006352

54. Huang SP (2004) Merging information from different resources for new insights into climate change in the past and future. Geophysical Research Letters 31: L13205. doi: 10.1029/2004gl019781

55. Mann ME, Bradley RS, Hughes MK (1999) Northern hemisphere temperatures during the past millennium: Inferences, uncertainties, and limitations. Geophysical Research Letters 26: 759–762.

56. Shi F, Yang B, Mairesse A, von Gunten L, Li JP, Brauning A, et al. (2013) Northern Hemisphere temperature reconstruction during the last millennium using multiple annual proxies. Climate Research 56: 231–244.

57. Shi N, Liu WB, Miao ZS (1989) The relationship between the SO and monthly or seasonal mean temperature in China. Meteorological Monthly 15: 8–13. [in Chinese, with English abstract]

58. Song J (1998) Reconstruction of the southern oscillation from dryness/wetness in China for the last 500 years. International Journal of Climatology 18: 1345–1355.

59. Fu CB, Jiang ZH, Guan ZY, He JH, Xu ZF (2008) Regional Climate Studies of China. Berlin Heidelberg: Springer. 476 p.

60. Wang B (2006) The Asian Monsoon. Berlin Heidelberg: Springer. 787 p.

61. Jones PD, Jonsson T, Wheeler D (1997) Extension to the North Atlantic Oscillation using early instrumental pressure observations from Gibraltar and south-west Iceland. International Journal of Climatology 17: 1433–1450.

62. Mantua NJ, Hare SR, Zhang Y, Wallace JM, Francis RC (1997) A Pacific interdecadal climate oscillation with impacts on salmon production. Bulletin of the American Meteorological Society 78: 1069–1079.

63. Fang KY, Gou XH, Chen FH, Li JB, D'Arrigo R, Cook E, et al. (2010) Reconstructed droughts for the southeastern Tibetan Plateau over the past 568 years and its linkages to the Pacific and Atlantic Ocean climate variability. Climate Dynamics 35: 577–585.

64. Liu N, Liu Y, Zhou Q, Bao G (2013) Droughts and broad-scale climate variability reflected by temperature-sensitive tree growth in the Qinling Mountains, central China. International Journal of Biometeorology 57: 169–177. doi: 10.1007/s00484-012-0544-8 PMID: 22527758

65. Chen ZS, Chen YN, Bai L, Xu JH (2016) Multiscale evolution of surface air temperature in the arid region of Northwest China and its linkages to ocean oscillations. Theoretical and Applied Climatology. doi: 10.1007/s00704-016-1752-7

66. Li BF, Chen YN, Shi X (2012) Why does the temperature rise faster in the arid region of northwest China? Journal of Geophysical Research-Atmospheres 117: D16115. doi: 10.1029/2012JD017953

67. Feldstein SB (2003) The dynamics of NAO teleconnection pattern growth and decay. Quarterly Journal of the Royal Meteorological Society 129: 901–924.

68. Watanabe M (2004) Asian jet waveguide and a downstream extension of the North Atlantic Oscillation. Journal of Climate 17: 4674–4691.

69. Sun JQ, Wang HJ, Yuan W (2008) Decadal variations of the relationship between the summer North Atlantic Oscillation and middle East Asian air temperature. Journal of Geophysical Research-Atmospheres 113: D15107. doi: 10.1029/2007JD009626

70. Robock A (2000) Volcanic eruptions and climate. Reviews of Geophysics 38: 191–219.

71. D'Arrigo RD, Jacoby GC (1999) Northern North American tree-ring evidence for regional temperature changes after major volcanic events. Climatic Change 41: 1–15.

72. Gervais BR, MacDonald GM (2001) Tree-ring and summer-temperature response to volcanic aerosol forcing at the northern tree-line, Kola Peninsula, Russia. Holocene 11: 499–505.

73. Siebert L, Simkin T (2012) Volcanoes of the World: An Illustrated Catalog of Holocene Volcanoes and Their Eruptions. Global Volcanism Program Digital Information Series: Smithsonian Institution.

74. Jia PQ, Shi GQ (2001) Study on the effects of volcanic eruption and solar activityon climate in China in recent 50 years. Plateau Meteorology 20: 225–233. [in Chinese, with English abstract].

75. Li JB, Xie SP, Cook ER, Morales MS, Christie DA, Johnson NC, et al. (2013) El Nino modulations over the past seven centuries. Nature Climate Change 3: 822–826.